

Article

The Isotopic ($\delta^{18}\text{O}$, $\delta^2\text{H}$, $\delta^{13}\text{C}$, $\delta^{15}\text{N}$, $\delta^{34}\text{S}$, $^{87}\text{Sr}/^{86}\text{Sr}$, $\delta^{11}\text{B}$) Composition of Adige River Water Records Natural and Anthropogenic Processes

Chiara Marchina ¹, Kay Knöller ², Maddalena Pennisi ³, Claudio Natali ⁴ , Marlene Dordoni ³, Paolo Di Giuseppe ³, Rosa Cidu ⁵ and Gianluca Bianchini ^{1,*} 

¹ Department of Physics and Earth Sciences, University of Ferrara, 44121 Ferrara, Italy; mrcchr@unife.it

² Department of Catchment Hydrology, Helmholtz Centre for Environmental Research, UFZ, Halle/Saale, 04318 Leipzig, Germany; kay.knoeller@ufz.de

³ Institute of Geosciences and Earth Resources (IGG), National Research Council (CNR), 56124 Pisa, Italy; m.pennisi@igg.cnr.it (M.P.); mvdordoni@gmail.com (M.D.); paolo.digiuseppe@igg.cnr.it (P.D.G.)

⁴ Department of Earth Sciences, University of Florence, 50121 Florence, Italy; claudio.natali@unifi.it

⁵ Department of Chemical and Geological Sciences, University of Cagliari, 9124 Cagliari, Italy; cidur@unica.it

* Correspondence: bncglc@unife.it

Received: 27 March 2020; Accepted: 14 May 2020; Published: 18 May 2020



Abstract: The water composition of the river Adige displays a Ca–HCO₃ hydrochemical facies, mainly due to rock weathering. Nitrate is the only component that has increased in relation to growing anthropogenic inputs. The aim of this paper was to identify the origin of the dissolved components in this river and to establish the relationship between these components and critical zone processes within an evolving framework where climatic and human impacts are influencing the riverine system. In particular, emphasis is given to a wide spectrum of isotope data ($\delta^{18}\text{O}$, $\delta^2\text{H}$, $\delta^{13}\text{C}$, $\delta^{15}\text{N}$, $\delta^{34}\text{S}$, $^{87}\text{Sr}/^{86}\text{Sr}$, $\delta^{11}\text{B}$), which is considered useful for determining water origin as well as natural and anthropogenic impacts on riverine geochemistry. Together with oxygen and hydrogen isotopes, which are strictly related to the climatic conditions (precipitation, temperature, humidity), the carbon, sulphur, strontium and boron signatures can describe the magnitude of rock weathering, which is in turn linked to the climatic parameters. $\delta^{13}\text{C}_{\text{DIC}}$ varies regularly along the riverine profile between -4.5‰ and -9.5‰ , and $\delta^{34}\text{S}_{\text{SO}_4}$ varies regularly between $+4.4\text{‰}$ and $+11.4\text{‰}$. On the other hand, $\delta^{15}\text{N}_{\text{NO}_3}$ shows a more scattered distribution between $+3.9\text{‰}$ and $+10.5\text{‰}$, with sharp variations along the riverine profile. $^{87}\text{Sr}/^{86}\text{Sr}$ varies between 0.72797 in the upper part of the catchment and 0.71068 in the lower part. $\delta^{11}\text{B}$ also shows a rough trend, with values approaching 7.6‰ in the upper part and 8.5‰ in the lower part. In our view, the comparatively low $\delta^{34}\text{S}$, $\delta^{11}\text{B}$, and high $^{87}\text{Sr}/^{86}\text{Sr}$ values, could be a proxy for increasing silicate weathering, which is a process that is sensitive to increases in temperature.

Keywords: river geochemistry; rock weathering; geochemical fluxes; water isotopes; C–S–N isotopes; boron isotopes; strontium isotopes

1. Introduction

Water–rock interactions during weathering processes are essential for river geochemistry, and for understanding the elemental cycles between the lithosphere–pedosphere–atmosphere–hydrosphere [1–4] in the Earth’s skin, which is defined as the critical zone (CZ) [5,6]. This is very important because riverine systems represent a crucial source of freshwater and nutrients for both the continents and the oceans, as well as being ecological corridors for biological species [7].

Unfortunately, riverine ecosystems are often threatened by climatic changes and anthropogenic forces [8]. In particular, in the Mediterranean area, rivers are currently affected by a significant reduction in discharge, which is estimated to have decreased by 20% between 1960 and 2000 [9]. The decrease in river discharge appears to be caused by regional decreases in precipitation and increases in temperature linked to more general climate changes. This critical issue is particularly relevant for riverine systems fed by Alpine glaciers and the associated ecosystems [10,11].

The decrease in the water flux does not necessarily imply a reduction in elemental fluxes, as dissolved components are related to the weathering processes of bedrocks and soils, which can increase with increasing temperature in a climate change scenario, and are also impacted by human activity. For this reason, geochemical investigations of rivers from Alpine regions are very important to trace the water–rock interaction processes, and more generally, the functioning and evolution of the CZ, including the responses to environmental modifications caused by both natural and human-induced forces [12].

Within this framework, we investigated the water geochemistry of the Adige river in order to understand the origin of dissolved components and to establish their relationships with CZ processes in an evolving framework, where climatic and human impacts are affecting the riverine system. In particular, emphasis was given to a wide spectrum of isotope data ($\delta^{18}\text{O}$, $\delta^2\text{H}$, $\delta^{13}\text{C}$, $\delta^{15}\text{N}$, $\delta^{34}\text{S}$, $^{87}\text{Sr}/^{86}\text{Sr}$, $\delta^{11}\text{B}$), as this type of data is useful for discriminating between natural and anthropogenic impacts on water geochemistry [2,4,13–17].

2. Study Area

2.1. Hydrological Features of the Drainage Catchment

The Adige river is the second most important Italian river in terms of length, water discharge, and catchment width. It drains the Southern and Eastern Alps, rising at 1586 m a.s.l. (above sea level) near the Resia Lake, and after a course of 409 km, enters the Adriatic Sea at Porto Fossone north of the Po river delta [15,16].

It covers an area of about 12,100 km² [18,19] and 91% of the basin is located in Alpine settings, including 185 glaciers covering about 212 km² that represent an important water supply, especially during warmer periods [20]. Of note, the mean annual discharge measured at the Trento S. Lorenzo station (185 m³/s), which is at the end of the mountainous part of the catchment, is comparable with that observed at Boara Polesine (202 m³/s), not far from the estuarine mouth [21,22].

Starting from its source, the Adige river flows generally E–W for ca. 70 km in the Adige–Passirio sub-basin and receives contributions from small mountainous sub-catchments characterised by glaciated areas [23]. After confluence with the Passirio river, which drains the northernmost part of the basin, the Adige main stream turns toward N–S and after 30 km reaches the town of Bolzano, where it is characterised by a mean annual discharge of 50 m³/s. A few kilometres south, the Adige stream path meets the confluence with the Isarco river, which is one of the main tributaries (mean annual discharge of 80 m³/s) draining about half (the whole N–E part) of the catchment (Isarco–Talvera–Rienza sub-basins), and is characterised by a mean altitude of 1750 m a.s.l. At Trento, the Adige meets the Noce river (mean annual discharge of 35 m³/s), which drains an area that is characterised by a significant mean elevation (1625 m a.s.l.) and by the presence of some important glaciers [24,25]. A few kilometres southward, the main stream receives the Avisio and Fersina rivers (mean annual discharge of 23.5 and 2.0 m³/s, respectively), which both drain the central-eastern parts of the basin, with mean altitudes of 1660 and 1099 m a.s.l., respectively. In this stretch, the Adige Valley is intensively cultivated. Southward at ca. 220 km from its source, the Adige stream path turns to the east and faces the alluvial plain deposits. Additional tributaries drain the Lessini Mountains (Adige–Chiampo sub-basin) and reach the confluence with the Adige river at ca. 280 km from the source. Further downstream, the river does not receive any other superficial water income, and the riverbed, confined within continuous embankments on both sides, progressively rises higher than the surrounding alluvial plain. Down flow

of Verona, the basin is narrowed down. Huge amounts of water are extracted in this section for irrigation, industry, and drinking water supplies [26–28].

The Adige river catchment is characterised by a continental climate, with a precipitation regime that is mainly influenced by western Atlantic airflows and southern circulation patterns [29]. These result in relatively dry winters with the maximum precipitation recorded during the spring and fall. A significant amount of the water budget is accumulated at higher elevations during winter in the form of snow, which undergoes melting that starts in spring. The mean annual precipitation in the distinct sub-basins is highly variable depending on catchment elevation, valley orientation, and the distance from orographic barriers. It varies from a minimum of 400–500 mm/year in Val Venosta to a maximum of 1600 mm/year at higher elevations, and in the valleys that open toward the floodplain (data from Adige river Basin Authority [30]). Consequently, the stream flow shows a typical Alpine regime with two peaks: one in spring due to snow melt, and one in autumn due to cyclonic storms, which are the main cause of flooding events. In the period from 1850–1950, eight flood events occurred in the Adige catchment [31].

2.2. Geological Setting

From a geological point of view, the catchment can be subdivided in three main tectonic zones that correspond to the Penninic, Austroalpine and Southalpine domains [21,26,32–34]. Within the first two domains, located in the north-eastern part of the basin, highly metamorphosed rocks, mainly of Palaeozoic age, are widespread. They consist of prevalent gneisses and schists, and subordinate quartzites, amphibolites, serpentinites, and marbles.

The Southalpine domain includes different geological formations: Palaeozoic phyllites and igneous effusive rocks (porphyries) of the volcanic Atesino complex, Mesozoic sedimentary rocks, and Tertiary volcanic–sedimentary rocks of the Lessini Mounts. Holocene alluvial deposits outcrop in the plain; these sediments often represent reworked glacial and fluvio-glacial deposits [18,26,34].

3. Sampling and Analytical Methods

Water samples were collected in May 2015 and August 2016 along the Adige river (Figure 1, Table 1) from its source to its outlet in the Adriatic Sea. The river catchment was subdivided into an upper part (UP), which corresponds to the mountainous sector, and a lower part (LP), which corresponds to the related alluvial plain, as suggested in Natali et al. [18]. The main criteria for selecting sampling sites was the ability to monitor the water geochemistry along the river profile, before/after the confluence of important tributaries, settlements and/or zones of important productive activities [35]. At each sampling site, coordinates were recorded by a portable global positioning system (GPS), to locate the sampling points and to set up future field surveys. Surface water was collected at a depth of 40–50 cm, where the river flow was efficient. Electrical conductivity (EC), pH, and temperature were directly measured in the field. Alkalinity (mainly related to HCO_3^-) was determined in situ using an HI 3811 alkalinity kit (Hanna Instruments, Villafranca Padovana, Italy).

Table 1. Adige river sampling sites, elemental and isotopic composition of the river water collected in May 2015 and August 2016. n.d.= not detected.

Location	Data	Latitude	Longitude	Source d.	$\delta^{18}\text{O}$	$\delta^2\text{H}$	$\delta^{13}\text{C}_{\text{DIC}}$	$\delta^{15}\text{N}_{\text{NO}_3}$	$\delta^{18}\text{O}_{\text{NO}_3}$	$\delta^{34}\text{S}_{\text{SO}_4}$	$\delta^{18}\text{O}_{\text{SO}_4}$	HCO_3^-	NO_3^-	SO_4^{2-}	B	$\delta^{11}\text{B}$	Sr	$^{87}\text{Sr}/^{86}\text{Sr}$
				Km	‰	‰	‰	‰	‰	‰	‰	mg/L	mg/L	mg/L	µg/L	‰	µg/L	
Resia (source)	10/05/15	46°44'24.3" N	10°33'01.1" E	0	-13.5	-98.4	-7.9	5.7	6.8	4.42	2.2	33	0.65	25.0			95.0	
S. Valentino alla Muta (BZ)	09/08/16	46°46' 31" N	10° 32' 2" E	0	-13.5	-97.2	-6.4	7.9	29.0	2.95	2.2	36		23.5	3.0	7.60	58.9	0.72797
Glorenza (BZ)	10/05/15	46°40'12.7" N	10°31'55.6" E	11	-13.8	-100	-4.5	4.0	3.0	11.4	10.8	69	0.96	82.8			610	
	09/08/16	46°40' 13" N	10°31' 6.0" E	11	-13.5	-96.6	-4.8	0.1	3.6	11.18	10.1	63	1.00	115.7			705	
Spondigna BZ	10/05/15	46°38' 07" N	10°36'24.6" E	18	-13.6	-99.6	-7.6	n.d.	n.d.	10.2	8.8	90	1.03	71.0			475	
	09/08/16	46°38' 08" N	10°36' 23" E	18	-13.5	-96.6	-8.6	4.6	6.1	8.76	6.8	78	0.14	89.1			412	
Tel BZ	10/05/15	46°40'37.2" N	11°05'06.4" E	55	-13.7	-99.9	-6.1	7.6	6.0	7.41	5.7	69	1.54	59.3			276	
	09/08/16	46°40' 37" N	11°05' 06" E	55	-13.6	-97.2	-6.1	3.9	10.4	5.52	2.9	45	1.01	65.8			183	0.71318
Andriano BZ	10/05/15	46°30'41.4" N	11°15'37.9" E	85	-12.9	-93.0	-6.8	n.d.	n.d.	6.63	5.4	48	1.64	33.6			147	
	09/08/16	46°52' 21" N	11°24' 60" E	85	-12.5	-88.5	-7.0	2.2	4.5	5.45	3.1	54	1.68	50.8			141	
Isarco - Bolzano	11/05/15	46°29'12.8" E	11°19'56" E	92	-12.3	-86.8	-8.0	3.9	5.9	7.45	7.0	72	1.52	13.0			116	
	09/08/16	46°28' 23.6" N	11°18'41.8" E	92	-11.7	-82.5	-8.6	5.1	3.4	4.09	4.6	66	0.15	20.9	4.1	7.40	121	
Vadena Nuova BZ	10/05/15	46°24'49.6" N	11°18'53.8" E	100	-12.4	-88.1	-6.8	4.9	5.6	6.18	6.5	66	1.70	14.6			114	
	09/08/16	46°41' 4" N	11°31' 52" E	100	-11.9	-83.2	-9.0	8.7	6.4	5.38	5.7	69	1.59	23.9			178	
S. Floriano BZ	10/05/15	46°17'13.3" N	11°14'17.8" E	115	-12.3	-88.1	-7.5	5.0	5.8	7.35	7.0	63	1.63	22.2			138	
	09/08/16	46°28' 7" N	11°23' 85" E	115	-11.9	-83.9	-7.3	3.4	2.6	6.82	6.2	60	1.15	34.4	7.3	8.40	134	0.71038
Zambana TN	10/05/15	46°9'20.3" N	11°5'24.6" E	135	-12.3	-87.8	-8.5	6.8	7.3	7.38	6.1	66	1.84	20.8			129	
	09/08/16	46°9' 19.6" N	11°5' 21.6" E	135	-11.9	-85.0	-8.1	4.3	3.5	5.84	4.4	60	1.57	33.3	5.5	7.00	150	0.71098
Mattarello TN	11/05/15	46°00'34.3" N	11°7'22.1" E	155	-12.2	-86.2	-8.7	7.4	7.4	7.23	6.4	63	1.41	21.1			131	
	09/08/16	46°00' 06" N	11°12' 33" E	155	-11.9	-83.4	-5.6	3.2	3.9	5.73	3.9	54	0.88	32.0			135	0.71059
Pilcalte TN	11/05/15	45°45'57.3" N	11°00'04.4" E	185	-12.1	-84.7	-9.0	6.9	6.0	7.71	5.8	87	2.57	22.0			146	
	10/08/16	45°76' 6" N	11°00' 14" E	185	-11.8	-81.4	-7.6	3.9	6.60	4.6	75	1.24	29.7	8.2	4.50	114		
Brentino Belluno VR	11/05/15	45°38'25.2" N	10°52'35" E	205	-12.1	-85.1	-9.0	6.2	5.3	7.15	5.4	90	1.98	20.4			130	
	10/08/16	45°65' 69" N	10°89' 43" E	205	-11.7	-81.0	-7.7	3.3	-0.4	6.70	5.5	81	1.04	29.5	7.0	7.10	131	
Parona VR	11/05/15	45°28'32.9" N	10°56'43.8" E	235	-11.9	-84.1	-9.3	7.0	8.6	6.95	6.1	84	2.46	19.7			139	
	10/08/16	45°46' 41" N	10°94' 10" E	235	-11.6	-80.3	-7.9	3.6	2.2	6.45	5.2	78	1.56	30.5	7.8	9.40	151	0.71071
Zevio VR	11/05/15	45°22'51.9" N	11°08'06.6" E	265	-12.1	-85.7	-8.9	10.5	7.7	7.22	5.2	69	n.d.	19.8			131	
	10/08/16	45°38' 13" N	11°13' 51" E	265	-11.7	-81.9	-7.5	4.0	3.8	6.56	5.5	78	1.97	32.3	8.2	9.10	149	0.71074
Bonavigo VR	11/05/15	45°12'51.3" N	11°17'52.3" E	290	-11.9	-83.6	-9.5	8.7	8.1	7.64	5.8	69	3.52	20.5			141	
	10/08/16	45°21' 4" N	11°29' 79" E	290	-11.6	-81.4	-7.9	5.8	2.3	6.85	5.3	81		32.2			163	
Badia Polesine RO	11/05/15	45°06'18" N	11°28'50.1" E	315	-11.8	-83.4	-8.3	8.6	8.0	7.71	6.4	84	3.70	20.1			140	
	10/08/16	45° 0' 49" N	11°48' 06" E	315	-11.6	-81.6	-7.8	6.8	2.4	6.55	6.0	87	0.61	32.5			146	
Boara Pisani RO	11/05/15	45°06' 34" N	11°47' 31" E	320	-12.1	-85.0	-9.4	6.4	4.6	7.61	6.2	78	3.08	20.7			185	
	10/08/16	45°06' 34" N	11°47' 31" E	320	-11.5	-81.1	-8.1	5.1	-0.1	6.52	5.4	78	1.41	31.2			122	
Rosolina Mare RO	11/05/15	45°08'34.7" N	12°18'27.9" E	385	-12.1	-85.5	-9.0	6.2	2.9	7.87	6.4	78	n.d.	20.6			129	
	10/08/16	45°14' 29" N	12°30' 71" E	385	-11.5	-80.9	-8.8	6.2	2.4	6.32	5.3	75	0.88	31.1			148	

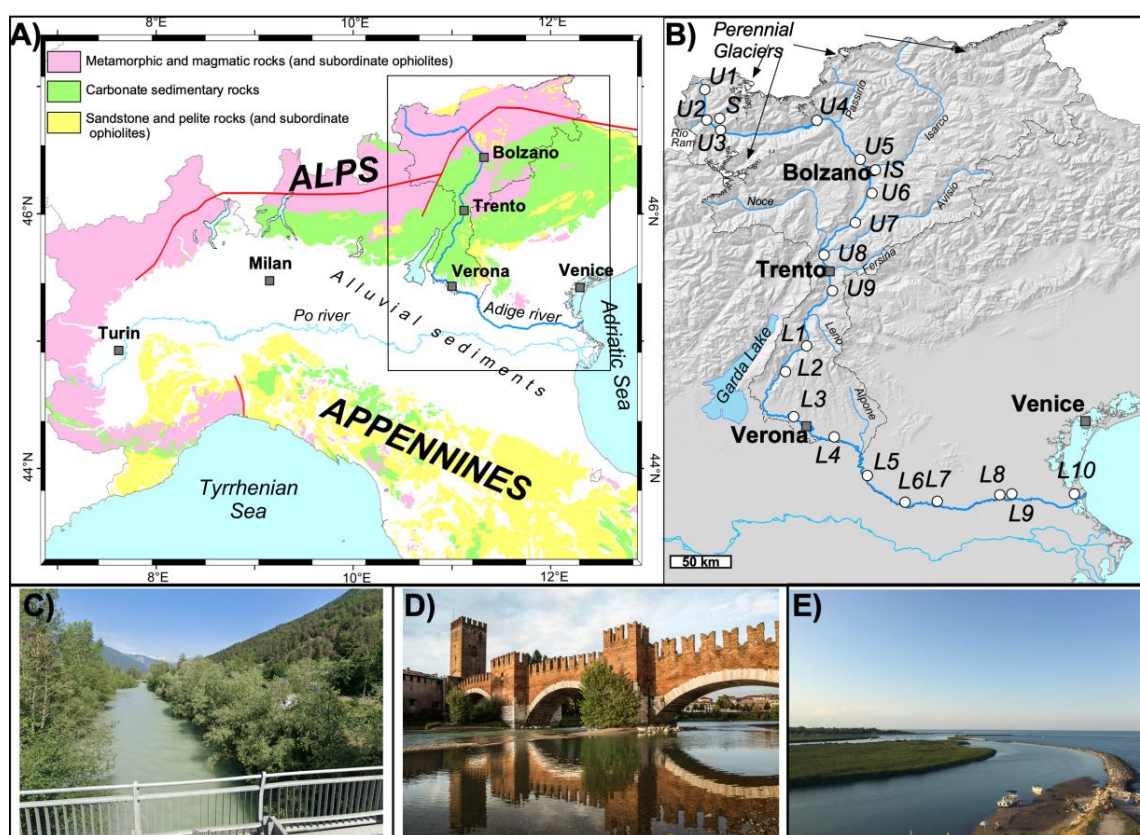


Figure 1. (A) Geological sketch map of northern Italy, modified by Natali et al. [18]; (B) Adige river catchment with sampling locations; (C) Adige river at Spondigna (BZ); (D) Adige river at Verona; (E) Adige river mouth at Rosolina.

For the analyses of anions and oxygen, hydrogen, carbon, sulphur, strontium, and boron isotopes, the water samples were filtered at $0.45\ \mu\text{m}$, whereas for nitrogen isotopic analysis, the water samples were filtered at $0.20\ \mu\text{m}$ (using Minisart[®] NML syringe cellulose acetate filters, Göttingen, Germany).

For the analyses of cations and trace elements, the water samples were filtered ($0.45\ \mu\text{m}$) and acidified with $0.5\ \text{mL}$ of concentrated Suprapure HNO_3 .

Chemical analyses and isotopic analyses of $\delta^2\text{H}$ and $\delta^{18}\text{O}$ were carried out at the Department of Physics and Earth Sciences of the University of Ferrara (Italy). Cations were measured by inductively coupled plasma mass spectrometry (ICP-MS), using a Thermo-Scientific X Series instrument (Thermo Fisher Scientific, Waltham, MA, USA). The anions were determined by ion chromatography, using a DIONEX ICS-1000 instrument (Thermo Fisher Scientific, Waltham, MA, USA). Accuracy and precision, based on repeated analyses of samples and standards, were better than 10% for all the considered parameters. Hydrogen and oxygen isotope ratios were analysed using a CRDS LWIA isotopic analyser (model 24-d, manufacturer by Los Gatos Research, San José, CA, USA), as described by Natali et al. [18].

Carbon, sulphur and nitrogen isotopes ($\delta^{13}\text{C}$, $\delta^{34}\text{S}$, $\delta^{15}\text{N}$) in the Adige river water were assessed in the laboratories of the Helmholtz Centre for Environmental Research Halle/Germany.

Isotope analyses of dissolved inorganic carbon were carried out in gaseous carbon dioxide directly liberated from the water samples with phosphoric acid [36]. This technique used helium flushed glass septum tubes pre-loaded with phosphoric acid. The water samples were injected into these septum tubes. CO_2 isotope measurements were performed using a Delta V plus isotope ratio mass spectrometer (IRMS) fitted with a Gasbench II, Thermo Electron GmbH. $^{13}\text{C}/^{12}\text{C}_{\text{DIC}}$ isotope ratios were reported with the δ notation, with respect to the Pee Dee Belemnite (PDB) international standard. Repeated analyses of standards (NBS-19) and samples revealed a $\delta^{13}\text{C}_{\text{DIC}}$ precision and accuracy

of 0.1‰. The associated $^{18}\text{O}/^{16}\text{O}_{\text{DIC}}$ were reported with the δ notation, with respect to the SMOW international standard.

Any dissolved sulfate in the water samples was precipitated as BaSO_4 by the addition of a 0.5 M BaCl_2 solution [37]. Sulfur isotopic compositions were measured after conversion of BaSO_4 to SO_2 using an elemental analyser (continuous flow flash combustion technique), coupled with a gas isotope ratio mass spectrometer (delta S, ThermoFinnigan, Bremen, Germany). Sulfur isotope measurements were performed with an analytical error of the measurement of better than $\pm 0.3\text{‰}$, and the results are reported in delta notation ($\delta^{34}\text{S}$) as the part per thousand (‰) deviation relative to the Vienna Cañon Diablo Troilite (VCDT) standard. Oxygen isotope analysis on barium sulfate samples was carried out by high temperature pyrolysis at 1450 °C in a thermal combustion elemental analyser (TC/EA) connected to a delta plus XL gas isotope ratio mass spectrometer (ThermoFinnigan), with an analytical error better than $\pm 0.5\text{‰}$. The results of oxygen isotope measurements are expressed in delta notation ($\delta^{18}\text{O}$) as the part per thousand (‰) deviation relative to the Vienna Standard Mean Ocean Water (V-SMOW). For normalising the $\delta^{34}\text{S}$ data, the IAEA-reference materials NBS 127 (BaSO_4) and IAEA-S1 (Ag_2S) were used. The assigned values were +20.3‰ (VCDT) for NBS 127 and 0.3‰ (VCDT) for IAEA-S1. The normalisation of the oxygen isotope data of sulfate was carried out using the reference material NBS 127 with an assigned $\delta^{18}\text{O}$ value of +8.7‰ (V-SMOW).

The nitrogen and oxygen isotope analyses of nitrate were conducted on a GasbenchII/delta V plus combination (Thermo Fisher Scientific, Waltham, MA, USA) using the denitrification method for the simultaneous determination of $\delta^{15}\text{N}$ and $\delta^{18}\text{O}$ in the measuring gas N_2O , produced by the controlled reduction of sample nitrate [38,39]. The nitrogen and oxygen isotope results are reported in delta notation ($\delta^{15}\text{N}$, $\delta^{18}\text{O}$) as the part per thousand (‰) deviation relative to the standard AIR for nitrogen and VSMOW for oxygen. The standard deviation of the described analytical measurement is $\pm 1.6\text{‰}$ for $\delta^{18}\text{O}$ and $\pm 0.4\text{‰}$ for $\delta^{15}\text{N}$. The isotope results represent the mean value of two measurements of each sample. For calibration of nitrogen and oxygen isotope values, the reference nitrates IAEA-N3 ($\delta^{15}\text{N}$: +4.7‰ AIR; $\delta^{18}\text{O}$: +25.6‰ VSMOW), USGS32 ($\delta^{15}\text{N}$: +180‰ AIR; $\delta^{18}\text{O}$: +25.7‰ VSMOW), USGS 34 ($\delta^{15}\text{N}$: -1.8‰ AIR; $\delta^{18}\text{O}$: -27.9‰ VSMOW), and USGS 35 ($\delta^{15}\text{N}$: +2.7‰ AIR; $\delta^{18}\text{O}$: +57.5‰ VSMOW) were used [40].

Isotope analyses of strontium ($^{87}\text{Sr}/^{86}\text{Sr}$) were performed at IGG-CNR Pisa (Italy). The water samples were treated in a 100–1000 class clean room using standard cation exchange chromatographic procedures. Sr was eluted with HNO_3 (0.05N) and analysed using a Multi Collector ICP-MS, Neptune PlusTM. The $^{87}\text{Sr}/^{86}\text{Sr}$ ratios were corrected for ^{84}Kr and ^{86}Kr , and normalised to $^{86}\text{Sr}/^{88}\text{Sr} = 0.1194$. Analyses of the NIST SRM 987 (SrCO_3) isotopic standard run at the same time gave an average $^{87}\text{Sr}/^{86}\text{Sr}$ value of 0.710242 ± 16 (2σ , $n = 6$).

The boron analyses were extremely challenging, both in terms of content and isotopic composition, due to the very low concentrations in the Adige samples. Elemental analyses of boron were carried out at the Cagliari University by repeated ICP-MS (PE- Elam DRC) analyses on undiluted samples; the relative standard deviation varied between 1.2% and 20.6%, which increased with decreasing B content.

For the isotopic analyses of boron, about 50–70 mL of water was processed in a 100–1000 class clean room. B was separated from the matrix using ion exchange procedures with Amberlite, and eluted using 2% HNO_3 . The $^{11}\text{B}/^{10}\text{B}$ was measured on a Neptune PlusTM using 1012 Ohm resistors. The MC-ICP-MS was first tuned for the most stable mass fractionation [41]. The $^{11}\text{B}/^{10}\text{B}$ ratio was determined with the bracketing method, using a 25 ppb solution of 951 NBS standard to correct the instrumental mass fractionation. For the analyses, the sample was run at a signal intensity close to the standard one. The results are expressed in the delta notation ($\delta^{11}\text{B}\text{‰}$) relative to the above-mentioned reference material (boric acid) 951 NBS [42]. Aliquots of B1, B2, and B3 -IAEA standards were treated as the samples, and $\delta^{11}\text{B}$ was determined. The average values of the IAEA standards [43,44] measured at IGG-CNR using a Neptune Plus were $39.7 \pm 0.6\text{‰}$ (n.9) for standard B1, $13.8 \pm 1.2\text{‰}$ (n.8) for standard B2 and $-21.4 \pm 0.7\text{‰}$ (n.7) for standard B3. Known samples, analysed using TIMS (VG-54E; at IGG-CNR) and MC-ICP-MS (Neptune Plus; at ALS Lulea), were also run on the Neptune Plus

at IGG-Pisa during this study. The samples covered a large range of fluid chemistry, B content and B-isotope compositions [45,46].

4. Results

4.1. Chemical Composition of the Adige River Dissolved Loads

In the Supplementary Materials, Table S1 reports the chemical composition of the Adige river water, with the total dissolved solids (TDS) varying from 45 mg/L and 424 mg/L and Ca–HCO₃ hydrochemical facies. Supplementary Materials Figure S1, reports data from this study and previous papers [18,34] plotted as box plots, which demonstrate the relative constancy of most dissolved components. The concentration of the major ions is very low in the pristine waters draining through metamorphic rocks (silicate composition) in the initial part of the river, but drastically increases at the confluence with the Rio Ram stream, a tributary draining through sedimentary rocks. Then, down flow, the concentration slowly decreases because the successive tributaries have catchments dominated by metamorphic silicate rocks that are scarcely weathered. At the end of the mountainous part of the catchment, after the confluence with the Isarco river, the Adige river water assumes a geochemical constancy that is maintained for the whole river path, except in the terminal part of the river, which is influenced by marine components. It is interesting to note that the concentrations of most major dissolved components (excepted calcium and nitrates) are comparable to those observed in the Adige river water more than fifty years ago when anthropogenic inputs were probably less marked than nowadays [47,48].

4.2. Water Stable Isotopes ($\delta^2\text{H}$, $\delta^{18}\text{O}$)

The oxygen and hydrogen stable isotopes of Adige river water are reported in Table 1. These parameters are sensitive indicators of temperature and humidity at the regional scale, and their monitoring is essential to the understanding of climatic changes [11–16,49,50]. For the samples considered in this study, the values refer to distinct sampling periods, plotted as $\delta^{18}\text{O}$ vs. the distance from the source, as shown in a diagram that displays sub-parallel trends (Figure 2A). Samples collected in May 2015 show more negative values, which were partially the result of snow/ice-melt whereas the samples of August 2016 were influenced by summer rains, as they were sampled during a period of meteoric precipitation in the UP of the catchment (120 mm of rain in the two weeks before the sampling) that increased the water budget and the river discharge.

Oxygen isotopes of the studied water were plotted vs. the relative hydrogen isotopes in Figure 2A, together with data from the literature on the river Adige. The recorded $\delta^{18}\text{O}$ – $\delta^2\text{H}$ values of Adige river water lie close to the local meteoric water line [49], and do not reveal significant signs of evaporation. In fact, the river water line (RWL) of 2015 (reported in Table S2 in the Supplementary Materials and computed using ordinary least square regression) has a slope of 7.9 (n.33, $R^2 = 0.94$), whereas the RWL of 2016 has a slope of 7.4 (n.28, $R^2 = 0.92$). Only in September 2016 and July 2017 did Adige river water show less negative values [34] and a larger deviation from the local meteoric water line, which highlight slight evaporative effects. However, the Adige river system is more resilient to annual climate changes compared to other river systems (possibly because its glacio-nival regime delays the isotopic response, [18]), and statistical parameters reported in Supplementary Materials, Table S2 show that the heaviest isotopic compositions in the time series 2013–2017 were recorded in 2015 and 2017, which were the warmest and the driest in the last 50 years, respectively.

The d-excess values, calculated with respect to the global meteoric water line (GMWL) [51], as $d\text{-exc} = \delta^2\text{H} - 8 \times \delta^{18}\text{O}$ varies from 10.3 to 15.3 in the two sampling periods, in agreement with the d-excess values reported for other Italian large-scale catchments [15,50,52]; this parameter shows that the recharge is linked to precipitation in both the Atlantic (low d-excess) and Mediterranean provenance (high d-excess).

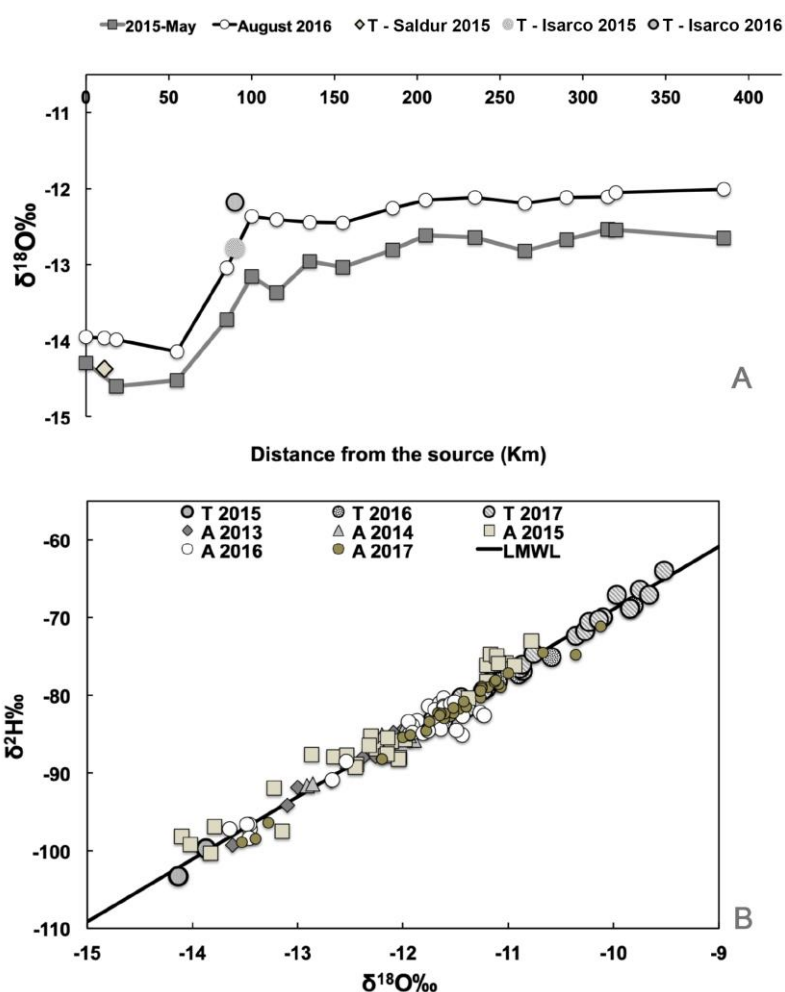


Figure 2. (A) Spatial variation in the $\delta^{18}\text{O}$ of Adige river water from the source to the estuary, recorded in May 2015 [18] and August 2016; (B) $\delta^{18}\text{O}$ – $\delta^2\text{H}$ of Adige river water (A), the main tributaries (T) and the meteoric water lines defined for northern Italy by Giustini et al. [49]. The reported values are the original data presented in this study (Table 1) supplemented by data from the literature [18–34].

4.3. Carbon, Sulphur and Nitrogen Isotopic Composition of Dissolved Components

The carbon, sulphur and nitrogen isotopic compositions of the dissolved components are reported in Table 1 and Figure 3.

As shown in Figure 3A, the variation in $\delta^{13}\text{C}_{\text{DIC}}$ is scattered in the first part of the river, down to Trento station (≈ 155 km from the source). In fact, in the upper course the recorded $\delta^{13}\text{C}_{\text{DIC}}$ value varies from -7.9 ‰ at the source to -4.5 ‰ after 11 km (i.e., after the confluence of the Rio Ram torrent, which drains through sedimentary rocks), then reaches -7.6 ‰ at Spondigna (after 18 km). These isotopic values in the first part of the river appeared to be constant in the two investigated periods. Down flow, after Trento, the carbon isotopic signatures become more stable, with the values in May 2015 being lower than those in August 2016 (average $\delta^{13}\text{C}_{\text{DIC}} = -9$ ‰ and average $\delta^{13}\text{C}_{\text{DIC}} = -7.9$ ‰, respectively), possibly in relation to the attainment of CaCO_3 saturation that buffered further changes. These values are on average less negative (by about 2‰) than those observed in the Po river main course. In Figure 4, the $\delta^{13}\text{C}_{\text{DIC}}$ measured in the Adige river water was compared with the HCO_3^- , and showed intermediate values between the reference line for an open system equilibrium between DIC and atmospheric CO_2 and that expected for non-equilibrium dissolution of carbonates proposed by Barth et al. [53].

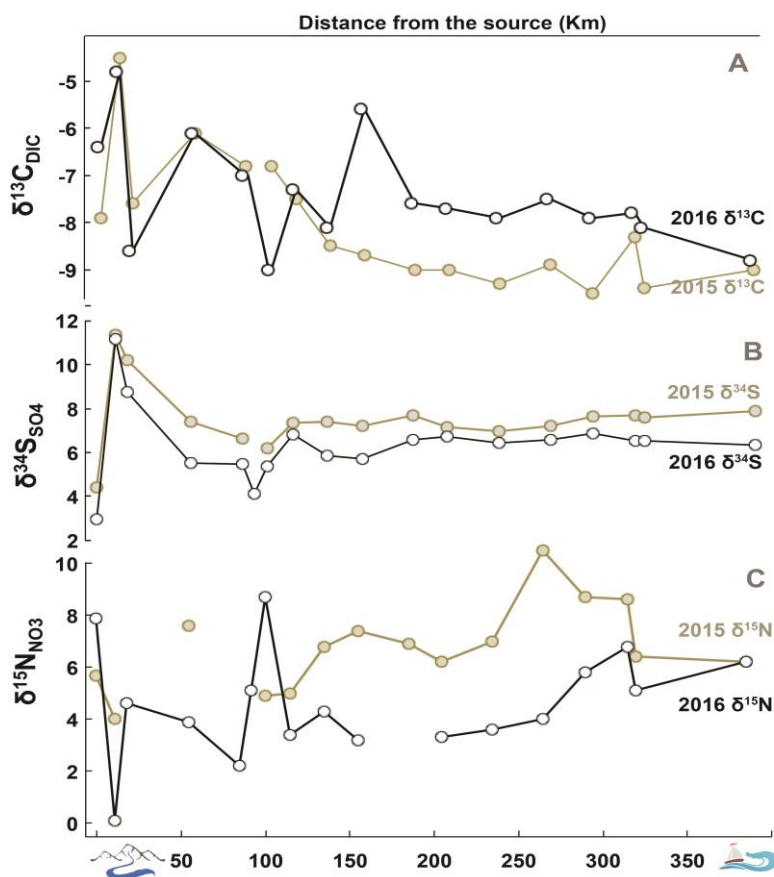


Figure 3. Spatial variations in the (A) $\delta^{13}\text{C}_{\text{DIC}}$, (B) $\delta^{34}\text{S}_{\text{SO}_4}$, (C) $\delta^{15}\text{N}_{\text{NO}_3}$ of Adige river water collected in May 2015 and August 2016.

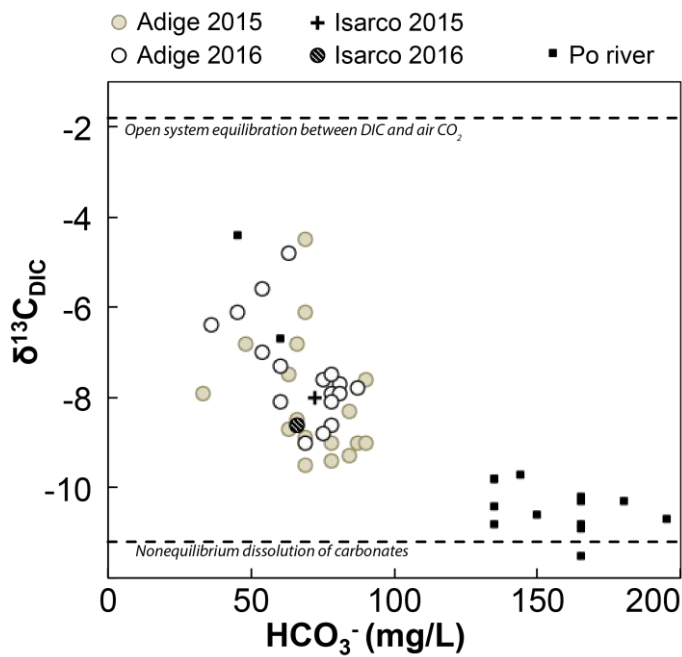


Figure 4. HCO_3^- and $\delta^{13}\text{C}_{\text{DIC}}$ measured in Adige river water compared with Po river water from Marchina et al. [16], and the isotopic compositions expected for open system equilibrium between DIC and atmospheric CO_2 and that expected for non-equilibrium dissolution of carbonates [53].

Figure 3B shows spatial variations in the $\delta^{34}\text{S}_{\text{SO}_4}$ of the Adige river water from the source to the Adriatic Sea in the two different periods, together with the values for the Isarco tributary. The UP of the Adige river (up to 50 km) shows values of $\delta^{34}\text{S}_{\text{SO}_4}$ between 4‰ at the source and 11‰ after 11 km (i.e., after the confluence of the Rio Ram torrent that drains through sedimentary rocks, including sulphates). Down flow, after 18 km, the $\delta^{34}\text{S}_{\text{SO}_4}$ decreases and then attains an average value of 7.5‰.

Figure 5A shows a weak correlation between SO_4^{2-} and $\delta^{34}\text{S}_{\text{SO}_4}$, with an R^2 of 0.54 and 0.59 for samples collected in May 2015 and August 2016, respectively. This plot highlights significant differences between samples from the UP of the river, in the first 50 km from the source; the Adige source is characterised by low SO_4^{2-} and low $\delta^{34}\text{S}_{\text{SO}_4}$ (25 mg/L and 4.4‰ in May 2015 and 23.5 mg/L and 2.95‰ in August 2016), but samples collected after 11–18 km and 55 km are characterised by higher SO_4^{2-} and relatively high $\delta^{34}\text{S}_{\text{SO}_4}$. Compared with the Po river [16], Adige river water is enriched in SO_4^{2-} and have a more variable isotopic composition.

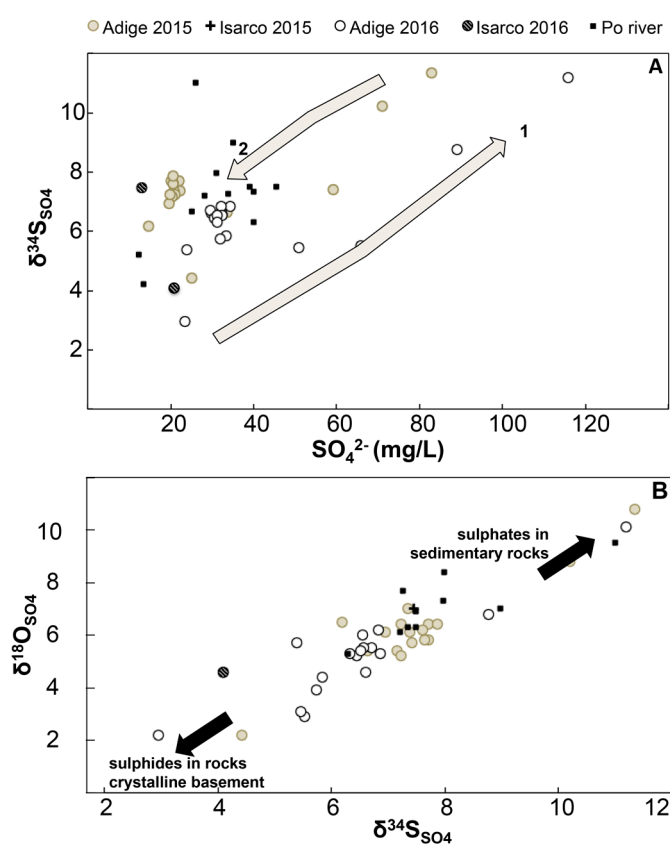


Figure 5. (A) SO_4^{2-} vs. $\delta^{34}\text{S}_{\text{SO}_4}$ diagram reporting the sulphate concentration and the relative $\delta^{34}\text{S}$ of Adige river water and the Isarco tributary. Arrow 1 represents the evolution observed in the first 11 km of the Adige course; arrow 2 represents the evolution toward a more mature river water composition observed in most of the river course. The Po river water samples are also represented; (B) $\delta^{34}\text{S}_{\text{SO}_4}$ vs. $\delta^{18}\text{O}_{\text{SO}_4}$ in Adige river water. The arrows indicate possible geogenic sources.

The plot of $\delta^{34}\text{S}_{\text{SO}_4}$ vs. $\delta^{18}\text{O}_{\text{SO}_4}$ (Figure 5B), which displays the correlation with $R_2 = 0.82$ and slope = 0.97, is useful to delineate the origin of sulphate in Adige river water. In the two different periods, the Adige river source was characterised by low sulphate concentration and low $\delta^{34}\text{S}_{\text{SO}_4}$, possibly indicating contributions from sulphides included in the crystalline basement, whereas the waters collected further down had higher sulphate concentrations and higher $\delta^{34}\text{S}_{\text{SO}_4}$ and $\delta^{18}\text{O}_{\text{SO}_4}$, indicating the contributions of sulphate-bearing carbonate lithologies [54]. After the high values observed at the confluences of Rio Ram, the $\delta^{34}\text{S}_{\text{SO}_4}$ and the relative SO_4^{2-} concentrations decrease, possibly indicating dilution of the Rio Ram signature by other water draining into the sulphide-bearing

basement in this area, or the influence of soil organic matter [55–57]. As previously observed in other important rivers, like the Arno river (Tuscany) [58], the Adige acts as a “homogenising container” and provides a weighted mean $\delta^{34}\text{S}_{\text{SO}_4}$ value of +7‰ for geogenic SO_4^{2-} in the catchment. Evidence of anthropogenic sulphate was not found in this work, as supported by the lack of correlation of SO_4^{2-} and NO_3^- .

Spatial variation in the $\delta^{15}\text{N}_{\text{NO}_3}$ of the Adige river water from the source to the sea in the two different periods is reported in Figure 3C, and Isarco is also represented. The two different periods are characterised by systematic isotopic differences: samples collected in May recorded $\delta^{15}\text{N}_{\text{NO}_3}$ higher than those collected in August 2016, and the summer isotopic values presented a more irregular distribution.

Nitrate elemental (NO_3^-) and isotopic ($\delta^{15}\text{N}_{\text{NO}_3}$) compositions of the Adige river water have been reported to show the compositional variation of nitrates in the surface water system (Figure 6A). Nitrates displayed relatively low concentrations in most of the samples collected (between 0.1 mg/L and 3.7 mg/L). Samples collected in May 2015 had higher values of nitrate (3.1 mg/L) compared to samples collected in August 2016 (1.4 mg/L). The isotopic value $\delta^{15}\text{N}_{\text{NO}_3}$ was in line with the isotopic signature of the groundwater and surface water in the Po plains [16,59,60].

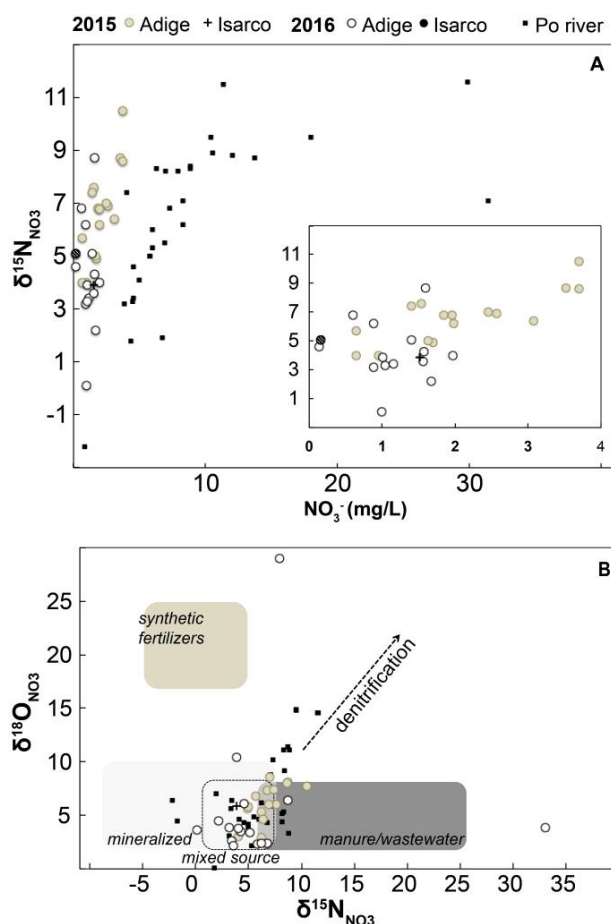


Figure 6. (A) NO_3^- and the relative isotopic composition ($\delta^{15}\text{N}_{\text{NO}_3}$) of Adige river water compared with the Po river water described Marchina et al. [16]. The inset shows the NO_3^- and $\delta^{15}\text{N}_{\text{NO}_3}$ of only the Adige river in the two different periods; (B) $\delta^{15}\text{N}_{\text{NO}_3}$ vs. $\delta^{18}\text{O}_{\text{NO}_3}$ plot reporting the isotopic value of the samples collected in May 2015 and August 2016 in the Adige river and Isarco tributary. Data are compared with the typical ranges of synthetic fertilizers, manure, wastewaters and soil organic matter [59,60] in order to provide specific information about natural/anthropogenic sources of dissolved nitrates.

In Figure 6B, where $\delta^{15}\text{N}_{\text{NO}_3}$ and $\delta^{18}\text{O}_{\text{NO}_3}$ are reported, the isotopic signature of the Adige river water conforms to mixed source/soil organic matter and manure, with higher isotopic values for samples collected in May 2015. Isotopic compositions vs. NO_3^- show a pattern that is similar to that recorded in the Po river water ($\delta^{15}\text{N}_{\text{NO}_3} \approx 5.1\text{‰}$; $\delta^{18}\text{O}_{\text{NO}_3} \approx 6\text{‰}$; [16]), despite NO_3^- values that are significantly lower ($0.15 \div 3.7 \text{ mg/L}$) in the Adige with respect to the Po river (up to 30 mg/L).

4.4. Strontium and Boron Isotopic Composition of Dissolved Components

The strontium and boron isotopic composition of Adige river water are reported in Table 1, and displayed in Figure 7 and Figures S2–S4.

The sample collected at the source of the Adige river was characterised by low Sr concentration (60 $\mu\text{g/L}$), with the highest $^{87}\text{Sr}/^{86}\text{Sr}$ ratio (0.72797). This is probably due to the contribution from the weathering of metamorphic rocks of the basement, which are predominant in the upper part of the basin. Then, the Sr concentration increased up to 700 $\mu\text{g/L}$, probably reflecting the confluence of the Rio Ram. Down flow, after 100 km from the source, the Sr concentration became rather homogeneous (because the river acts as a homogenising container, as observed for sulphate) and the relative $^{87}\text{Sr}/^{86}\text{Sr}$ attained the value of 0.71068, suggesting a higher contribution from carbonate rocks (Figure S2). If compared with the Po river (average composition 0.70922 [4]), the Adige river water appeared generally more radiogenic, with $^{87}\text{Sr}/^{86}\text{Sr}$ on average reaching 0.71351 (if we consider the source) or 0.71110 (if we do not consider the most radiogenic value at the source).

Boron displayed a very low elemental concentration, varying between 3 $\mu\text{g/L}$ (at the Adige source, Figure S3) and 8 $\mu\text{g/L}$ (after the city of Verona). This low boron content appears to be a common feature of alpine basins (e.g., Po; [59,60]). The $\delta^{11}\text{B}$ also showed a rough trend, with values approaching 7.6‰ in the UP and 8.5‰ in the lower part. Local precipitation ($\text{B} < 1 \text{ ppb}$, Supplementary Materials, Table S2) was also considered for B in this study. With the exclusion of one sample with a $\delta^{11}\text{B}$ of +24.3‰, the isotopic signature of boron in meteoric waters ranged from +7.3‰ to +11.8‰, which is in the range of the Adige river water; however, a B-source other than rain water has to be inferred, given the significant increase in B content recorded in the Adige river water. A B-source related to anthropogenic activities could be associated with the nitrate input, as it is generally accepted that B and NO_3^- are co-migrating tracers and useful indicators of anthropogenic pollution [59,61]. However, the widespread distribution of the investigated samples along the river course shows that the correlation between boron and nitrate in the Adige river is poor ($R^2 = 0.2$), and we can say that both the meteoric and the anthropogenic components could be considered as subordinate B-sources in the Adige river water. Therefore, the B-budget is mainly considered to be the result of water–rock interaction processes. In this view, the sample with the lowest boron isotopic composition (4.5‰) is likely related to the contribution of the Fersina stream, draining through crystalline rocks and volcanic rocks of rhyolite composition, with $\delta^{11}\text{B}$ values ranging from -20 to $+10\text{‰}$ [62]. The higher $\delta^{11}\text{B}$ of the samples (up to 9.4‰) could be related to groundwater hosted in carbonate-bearing matrices, with $\delta^{11}\text{B}$ values of up to +25‰ [63,64], as was also indicated by $^{87}\text{Sr}/^{86}\text{Sr}$. Indeed, groundwater inflating the river at the interface between the UP and the LP of the basin has been documented in the meandering segment of the Adige river, within the sampling site of Parona [18]. Indeed, the homogenising container represented by the Adige river has, when looking at B, an average $\delta^{11}\text{B}$ signature of $7 \pm 3\text{‰}$, which is mainly derived from water/rock interactions with crystalline and carbonate rocks (Figure 7).

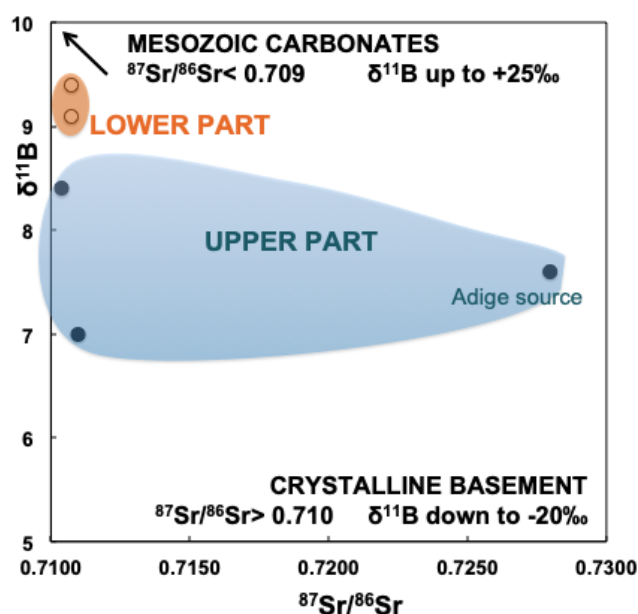


Figure 7. $^{87}\text{Sr}/^{86}\text{Sr}$ and $\delta^{11}\text{B}$ in Adige river water compared with the isotopic fingerprint of crystalline rocks of the basement and Mesozoic carbonates [65–68].

5. Discussion and Conclusions

To the best of our knowledge, the current paper reports for the first time, a data set that includes oxygen, hydrogen, carbon, nitrogen, sulphur, strontium and boron isotopes in the water of the Adige river.

The spatial distribution of $\delta^{18}\text{O}$ and $\delta^2\text{H}$ from the mountainous sector of the catchment down to the low part of the plain shows progressively less negative isotopic values down flow. The magnitude of the observed $\delta^{18}\text{O}$ and $\delta^2\text{H}$ variation progressively decreases in the first 100 km of UP, and the river progressively approaches a steady state condition in the remaining LP.

Carbon isotopes are variable along the UP of the river ($\delta^{13}\text{C}$ between -9‰ and -4.5‰), and their values are extremely sensitive to the various confluences of riverine systems draining through various lithologies. They become more homogeneous in the lower part of the river, where the average $\delta^{13}\text{C}$ value of -8.5‰ probably reflects the non-equilibrium weathering of carbonate rocks.

$\delta^{34}\text{S}_{\text{SO}_4}$ oscillates between 4‰ and 11‰ in the first 20 km of the river course and then attains an average value of 7.5‰ , which can be considered the result of contributions from both carbonate and silicate rocks.

The important role of silicate weathering was confirmed by the strontium isotopic composition that appears extremely radiogenic (up to 0.72797) if compared with the values recorded in the water of other important rivers draining from the Alps (Po, Danube, Rhine, Rhône [4]). The influence of silicate weathering decreases from the upper to the LP of the river, where the contribution of carbonate rocks gradually increases. This is also supported by the boron isotopic data, which show low values ($\delta^{11}\text{B}$ down to 4.5‰) in the UP of the river and progressively higher values down flow ($\delta^{11}\text{B}$ up to 9.4‰).

On the other hand, nitrogen has to be considered an anthropogenic component, and its isotopic signature reflects the source(s) of pollution. The $\delta^{15}\text{N}$ value of the Adige river water, with an average of 6.5‰ , reveals that nitrates derive from heterogeneous sources, such as manure and wastewater. The amount of nitrates in the Adige river is considerably lower (average of 2.3 mg/L at the Boara Polesine site) than the Po river (average of 8 mg/L , at the Pontelagoscuro site), but is generally in line with measurements along the river path reported by Chiogna et al. [34]. The Adige, together with the Po river, provides a significant flux of N-NO_3 to the Adriatic Sea that is variable in the different seasons depending on the discharge. In particular, nitrogen fluxes conveyed by the Adige river to the northern Adriatic Sea, calculated in daily campaigns in May 2015 and August 2016 at the Boara

Polesine site, are in the order of 13 t/day and 8 t/day, respectively. Thus, considering an average discharge of 202 m³/s [34] and an average NO₃ value of the two sampling campaigns, the total fluxes conveyed by the Adige river to the sea are in the order of 5.7 × 10³ t/year, which, added to the Po river fluxes [16], amounts to 113 × 10³ t/year. This evaluation of reactive dissolved nitrogen fluxes could be underestimated because a significant amount of this element is associated with suspended particulates [16,69].

In summary, the data reported above suggest that the elemental and isotopic composition of Adige river water is dominated by water–rock interactions occurring in the CZ. Together with oxygen and hydrogen isotopes that are strictly related to the climatic conditions (precipitation, temperature, humidity, [70]), the carbon, sulphur, strontium and boron signatures describe the magnitude of rock weathering, which is in turn linked to the climatic parameters. In this framework, we conclude that the comparatively low δ³⁴S and δ¹¹B coupled with the very high ⁸⁷Sr/⁸⁶Sr (which is higher than other important Alpine rivers [4]) are a proxy for significant silicate weathering, a process that is sensitive to increases in temperature. As the geochemical fingerprint of dissolved elements is dominated by geogenic components, the presented data can also contribute to calculations of geochemical fluxes conveyed by the Adige river into the Adriatic Sea.

In Supplementary Materials, Table S3, the geochemical fluxes have been calculated in different hydrological conditions, and this highlights the variability of the dissolved fraction conveyed by the river to the Adriatic Sea. Considering that the annual Adige water volume is 6.3 km³, the observed TDS (average of the TDS in Supplementary Materials, Table S3) implies a solute flux in the order of 1.3 × 10⁶ t/year transferred from the Adige river to the Adriatic Sea. Assuming that the solutes represent a fraction (accounting for ca. 20% of the weathering products [71]), we estimated denudation (chemical weathering plus physical erosion) and mass transport of 6.6 × 10⁶ t/year within the Adige river drainage basin, which gives an indication of the effectiveness of the CZ exogenous processes.

The reported data provide a snapshot of the current situation that, if compared with future studies, could highlight the evolution trends of both geogenic and anthropogenic components in this river and its catchment.

Supplementary Materials: The following are available online at <http://www.mdpi.com/2075-163X/10/5/455/s1>, Table S1: In situ parameters and major ions of the Adige river waters collected in May 2015 and August 2016, Table S2: Boron isotopic composition (δ¹¹B) of rainfall collected at Pacengo di Lazise (VR) in the Adige river catchment, Table S3: Discharge and TDS values recorded at Boara Polesine site (RO), in the lower part of the Adige river catchment. Dissolved fluxes were also calculated from these data. Data recorded in August 2013, May 2014, March 2015, May 2015 are reported in Natali et al., [18]. Data recorded from September 2016–July 2017 are reported in Chiogna et al., 2018 [34], Figure S1: Composition of the main dissolved components along the River Adige flow path. Data used for this representation are from the present work and from previous papers by Natali et al. [18] and Chiogna et al. [34], Figure S2: Spatial variation of Strontium and relative isotopic composition (⁸⁷Sr/⁸⁶Sr) in Adige river water, Figure S3: Spatial variation of Boron and the relative isotopic composition (δ¹¹B) in Adige river water, Figure S4: Binary diagram reporting the 1/Sr and the relative isotopic composition ⁸⁷Sr/⁸⁶Sr of the Adige river waters presented in this paper together with the Po river waters [4] and the isotopic values of the main Alpine rivers [3]. A dashed green line represents the mixing between a carbonate water end member (low ⁸⁷Sr/⁸⁶Sr, Tagliamento river) and silicate water end member (high ⁸⁷Sr/⁸⁶Sr, Adige river source). The tables report the complete dataset for the chemical analyses of the studied water and isotopic analyses of B in precipitation discussed in this manuscript.

Author Contributions: Conceptualization, G.B. and M.P.; Methodology, G.B.; C.N., C.M.; Formal Analysis, M.D., C.M., P.D.G., R.C., K.K.; Investigation, C.N., C.M., G.B., K.K.; Supervision, G.B.; Data curation, C.M., M.D., G.B.; Writing—Original Draft Preparation, C.M. and G.B.; Writing—Review and Editing, C.M., G.B. and M.P.; Fundraising: G.B., M.P., K.K. All authors have read and agreed to the published version of the manuscript.

Funding: This research was supported by the University of Ferrara (Italy), the IGG-CNR, Pisa (Italy) and the Helmholtz Centre for Environmental Research, UFZ (Germany).

Acknowledgments: We are grateful to the anonymous reviewers for their constructive comments and suggestions.

Conflicts of Interest: The authors declare no conflict of interest.

References

1. Mackenzie, F.T.; Garrels, R.M. Chemical mass balance between rivers and oceans. *Am. J. Sci.* **1966**, *264*, 507–525. [[CrossRef](#)]
2. Gaillardet, J.; Dupré, B.; Louvat, P.; Allègre, C.J. Global silicate weathering and CO₂ consumption rates deduced from the chemistry of large rivers. *Chem. Geol.* **1999**, *159*, 3–30. [[CrossRef](#)]
3. Donnini, M.; Frondini, F.; Probst, J.-L.; Probst, A.; Cardellini, C.; Marchesini, I.; Guzzetti, F. Chemical weathering and consumption of atmospheric carbon dioxide in the Alpine region. *Glob. Planet. Chang.* **2016**, *136*, 65–81. [[CrossRef](#)]
4. Marchina, C.; Natali, C.; Fahnestock, M.F.; Pennisi, M.; Bryce, J.; Bianchini, G. Strontium isotopic composition of the Po river dissolved load: Insights into rock weathering in Northern Italy. *Appl. Geochem.* **2018**, *97*, 187–196. [[CrossRef](#)]
5. Anderson, S.P.; Blum, J.; Brantley, S.L.; Chadwick, O.; Chorover, J.; Derry, L.A.; Drever, J.I.; Hering, J.G.; Kirchner, J.W.; Kump, L.R.; et al. Proposed initiative would study Earth’s weathering engine. *Eos, Transactions. Am. Geophys. Union* **2004**, *85*, 265–269. [[CrossRef](#)]
6. Brantley, S.L.; Di Biase, R.A.; Russo, T.A.; Shi, Y.; Lin, H.; Davis, K.J.; Kaye, M.; Hill, L.; Kaye, J.; Eissenstat, D.M.; et al. Designing a suite of measurements to understand the critical zone. *Earth Surf. Dyn.* **2016**, *4*, 211–235. [[CrossRef](#)]
7. Garbin, S.; Celegon, E.A.; Fanton, P.; Botter, G. Hydrological controls on river network connectivity. *R. Soc. Open Sci.* **2019**, *6*, 181428. [[CrossRef](#)]
8. Dostdogru, F.; Kalin, L.; Wang, R.; Yen, H. Potential impacts of land use/cover and climate changes on ecologically relevant flows. *J. Hydrol.* **2020**, *584*, 124654. [[CrossRef](#)]
9. Ludwig, W.; Dumont, E.; Meybeck, M.; Heussner, S. River discharges of water and nutrients to the Mediterranean and Black Sea: Major drivers for ecosystem changes during past and future decades? *Prog. Ocean.* **2009**, *80*, 199–217. [[CrossRef](#)]
10. Leonelli, G.; Battipaglia, G.; Cherubini, P.; Saurer, M.; Siegwolf, R.T.W.; Maugeri, M.; Stenni, B.; Fumagalli, M.L.; Pelfini, M.; Maggi, V. Tree-ring $\delta^{18}\text{O}$ from an Alpine catchment reveals changes in glacier stream water inputs between 1980 and 2010. *Art. Antarct. Alp. Res.* **2019**, *51*, 250–264. [[CrossRef](#)]
11. Marchina, C.; Lencioni, L.; Paoli, F.; Rizzo, M.; Bianchini, G. Headwaters’ isotopic signature as a tracer of stream origins and climatic anomalies: Evidence from the Italian Alps in summer 2018. *Water* **2020**, *12*, 390. [[CrossRef](#)]
12. Fan, Y.; Grant, G.; Anderson, S.P. Water within, moving through, and shaping the Earth’s surface: Introducing a special issue on water in the critical zone. *Hydrol. Process.* **2019**. [[CrossRef](#)]
13. Nisi, B.; Buccianti, A.; Vaselli, O.; Perini, G.; Tassi, F.; Minissale, A.; Montegrossi, G. Hydrogeochemistry and strontium isotopes in the Arno River Basin (Tuscany, Italy): Constraints on natural controls by statistical modeling. *J. Hydrol.* **2008**, *360*, 166–183. [[CrossRef](#)]
14. Urresti-Estala, B.; Vadillo-Pérez, I.; Jiménez-Gavilán, P.; Soler, A.; Sánchez-García, D.; Carrasco-Cantos, F. Application of stable isotopes ($\delta^{34}\text{S-SO}_4$, $\delta^{18}\text{O-SO}_4$, $\delta^{15}\text{N-NO}_3$, $\delta^{18}\text{O-NO}_3$) to determine natural background and contamination sources in the Guadalhorce River Basin (southern Spain). *Sci. Total Environ.* **2015**, *506–507*, 46–57. [[CrossRef](#)]
15. Marchina, C.; Bianchini, G.; Natali, C.; Pennisi, M.; Colombani, N.; Tassinari, R.; Knöller, K. The Po river water from Monviso source to the Adriatic Sea (Italy): New insights from geochemical and isotopic ($^{18}\text{O}/^{16}\text{O}$ - $^2\text{H}/^1\text{H}$) data. *Environ. Sci. Poll. Res.* **2015**, *22*, 5184–5203. [[CrossRef](#)] [[PubMed](#)]
16. Marchina, C.; Bianchini, G.; Knöller, K.; Natali, C.; Pennisi, M.; Colombani, N. Natural and anthropogenic variations in the Po river waters (northern Italy): Insights from a multi-isotope approach. *Isot. Environ. Health Stud.* **2016**, *16*, 1–24. [[CrossRef](#)]
17. Omorinoye, O.A.; Assim, Z.B.; Jusoh, I.B.; Durumin Iya, N.I.; Umaru, I.J. Review of the sedimentological and geochemical approaches for environmental assessment of River Sadong, Samarahan-Asajaya District Sarawak, Malaysia. *Nat. Environ. Poll. Tech.* **2019**, *18*, 815–823.
18. Natali, C.; Bianchini, G.; Marchina, C.; Knöller, K. Geochemistry of the Adige River water from the Eastern Alps to the Adriatic Sea (Italy): Evidences for distinct hydrological components and water-rock interactions. *Environ. Sci. Pollut. Res.* **2016**, *23*, 11677–11694. [[CrossRef](#)]

19. Diamantini, E.; Lutz, S.R.; Mallucci, S.; Majone, B.; Merz, R.; Bellin, A. Driver detection of water quality trends in three large European river basins. *Sci. Total Environ.* **2018**, *612*, 49–62. [[CrossRef](#)]
20. Milner, A.M.; Brown, L.E.; Hannah, D.M. Hydroecological effects of shrinking glaciers. *Hydrol. Process* **2009**, *23*, 62–77. [[CrossRef](#)]
21. Autorità di Bacino del Fiume Adige. Bibliografia Geologica e Naturalistica on line. Available online: <http://www.bacino-adige.it> (accessed on 7 March 2020).
22. Scorpio, V.; Surian, N.; Cucato, M.; Dai Prá, E.; Zolezzi, G.; Comiti, F. Channel changes of the Adige River (Eastern Italian Alps) over the last 1000 years and identification of the historical fluvial corridor. *J. Maps* **2018**, *14*, 680–691. [[CrossRef](#)]
23. Penna, D.; Engel, M.; Mao, L.; Dell’Agnese, A.; Bertoldi, G.; Comiti, F. Tracer-based analysis of spatial and temporal variations of water sources in a glacierized catchment. *Hydrol. Earth Syst. Sci.* **2014**, *18*, 5271–5288. [[CrossRef](#)]
24. Chiogna, G.; Santoni, E.; Camin, F.; Tonon, A.; Majone, B.; Trenti, A.; Bellin, A. Stable isotope characterization of the Vermigliana catchment. *J. Hydrol.* **2014**, *509*, 295–305. [[CrossRef](#)]
25. Zuecco, G.; Carturan, L.; De Blasi, F.; Seppi, R.; Zanoner, T.; Penna, D.; Borga, M.; Carton, A.; Dalla Fontana, G. Understanding hydrological processes in glacierized catchments: Evidence and implications of highly variable isotopic and electrical conductivity data. *Hydrol. Process.* **2019**, *33*, 816–832. [[CrossRef](#)]
26. Chiogna, G.; Majone, B.; Cano Paoli, K.; Diamantini, E.; Stella, E.; Mallucci, S.; Lencioni, V.; Zandonai, F.; Bellin, A. A review of hydrological and chemical stressors in the Adige catchment and its ecological status. *Sci. Total Environ.* **2016**, *540*, 429–443. [[CrossRef](#)]
27. Navarro-Ortega, A.; Acuna, V.; Bellin, A.; Burek, P.; Cassiani, G.; Choukr-Allah, R. Managing the effects of multiple stressors on aquatic ecosystems under water scarcity. The GLOBAQUA project. *Sci. Total Environ.* **2015**, *503*, 3–9. [[CrossRef](#)]
28. Autorità di Bacino del Fiume Adige (ABFA). Quaderno sul Bilancio Idrico Superficiale di Primo Livello. Bacino Idrografico del Fiume Adige. Autorità di Bacino del Fiume Adige Trento. Trento. 2008. Available online: http://www.bacino-adige.it/studi_realizzati/bilancio_idrico/PDF/Quaderno%20bilancio%20idrico%20lug08.pdf (accessed on 7 March 2020).
29. Norbiato, D.; Borga, M.; Merz, R.; Blöschl, G.; Carton, A. Controls on event runoff coefficients in the eastern Italian Alps. *J. Hydrol.* **2009**, *375*, 312–325. [[CrossRef](#)]
30. Adige River Basin Authority. Available online: <http://www.bacino-adige.it> (accessed on 7 March 2020).
31. Marchese, E.; Scorpio, V.; Fuller, I.; McColl, S.; Comiti, F. Morphological changes in Alpine rivers following the end of the Little Ice Age. *Geomorphology* **2017**, *295*, 811–826. [[CrossRef](#)]
32. Möller, P.; Morteani, G.; Dulski, P. Anomalous gadolinium, cerium, and yttrium contents in the Adige and Isarco River waters and in the water of their tributaries (Provinces Trento and Bolzano/Bozen, NE Italy). *Acta Hydroch. Hydrobiol.* **2003**, *31*, 225–239. [[CrossRef](#)]
33. Piovan, S.; Mozzi, P.; Zecchin, M. The interplay between adjacent Adige and Po alluvial systems and deltas in the late Holocene (Northern Italy). *Gèomorphologie* **2012**, *18*, 427–440. [[CrossRef](#)]
34. Chiogna, G.; Skrobaneck, P.; Narany, T.S.; Ludwig, R.; Stumpp, C. Effects of the 2017 drought on isotopic and geochemical gradients in the Adige catchment, Italy. *Sci. Total Environ.* **2018**, *645*, 924–936. [[CrossRef](#)] [[PubMed](#)]
35. Huber García, V.; Meyer, S.; Kok, K.; Verweij, P.; Ludwig, R. Deriving spatially explicit water uses from land use change modelling results in four river basins across Europe. *Sci. Total Environ.* **2018**, *628–629*, 1079–1097. [[CrossRef](#)] [[PubMed](#)]
36. Atekwana, E.A.; Krishnamurthy, R.V. Seasonal variations of dissolved inorganic carbon and $\delta^{13}\text{C}$ of surface waters: Application of a modified gas evolution technique. *J. Hydrol.* **1998**, *205*, 265–278. [[CrossRef](#)]
37. Knöller, K.; Trettin, R.; Strauch, G. Sulphur cycling in the drinking water catchment area of Torgau–Mockritz (Germany): Insights from hydrochemical and stable isotope investigations. *Hydrol. Process.* **2005**, *19*, 3445–3465. [[CrossRef](#)]
38. Sigman, D.M.; Casciotti, K.L.; Andreani, M. Bacterial method for the nitrogen isotopic analysis of nitrate in seawater and freshwater. *Anal. Chem.* **2001**, *73*, 4145–4153. [[CrossRef](#)]
39. Casciotti, K.L.; Sigman, D.M.; Galanter, H.M. Measurement of the oxygen isotopic composition of nitrate in seawater and freshwater using the denitrifier method. *Anal. Chem.* **2002**, *74*, 4905–4912. [[CrossRef](#)]

40. Böhlke, J.K.; Krantz, D.E. Isotope geochemistry and chronology of offshore ground water beneath Indian River Bay, Delaware: US Geological Survey. *Water-Resour. Investig. Rep.* 2003. Available online: <http://pi.lib.uchicago.edu/1001/cat/bib/7242370> (accessed on 7 March 2020).
41. Foster, G.L. Seawater pH, pCO₂ and [CO₃²⁻] variations in the Caribbean Sea over the last 130 kyr: A boron isotope and B/Ca study of planktic foraminifera. *Earth Planet. Sci. Lett.* **2008**, *271*, 254–266. [[CrossRef](#)]
42. Catanzaro, E.J.; Champion, C.E.; Garner, E.L.; Marinenko, G.; Sappenfield, K.M.; Shields, W.R. Boric assay; isotopic, and assay standard reference materials. *USA Natl. Bur. Stan. Spec. Publ.* **1970**, *260*, 70.
43. Tonarini, S.; Pennisi, M.; Adorni-Braccesi, A.; Dini, A.; Ferrara, G.; Gonfiantini, R.; Gröning, M. Intercomparison of boron isotope and concentration measurements. Part I: Selection, preparation and homogeneity tests of the intercomparison materials. *Geostand. Newsl.* **2003**, *27*, 21–39. [[CrossRef](#)]
44. Gonfiantini, R.; Tonarini, S.; Gröning, M.; Adorni-Braccesi, A.; Al-Ammar, A.S.; Astner, M.; Deyhle, A. Intercomparison of boron isotope and concentration measurements. Part II: Evaluation of results. *Geostand. Newsl.* **2003**, *27*, 41–57. [[CrossRef](#)]
45. Pennisi, M.; Agostini, S.; Dini, A.; Dordoni, M.; Di Giuseppe, P.; Rielli, A.; Provenzale, A.; Rodushkin, I. Boron isotope analyses in fluid samples: PTIMS versus MC-ICP-MS (Neptune Plus). In Proceedings of the International Symposium on Isotope Hydrology: Advancing the Understanding of Water Cycle Processes CN-271, Vienna, Austria, 20–24 May 2019.
46. Dordoni, M.; Pennisi, M.; Di Giuseppe, P.; Rielli, A.; Natali, C.; Bianchini, G.; Marchina, C.; Cidu, R. Boron isotopic composition in fluvial and rain water from the Adige basin (Northern Italy). In Proceedings of the International Symposium on Isotope Hydrology: Advancing the Understanding of Water Cycle Processes CN-271, Vienna, Austria, 20–24 May 2019.
47. Fossato, V.U. Ricerche idrologiche e chimico-fisiche sul Fiume Adige a Boara Pisani. Giugno 1968–Giugno 1969. *Arch. Ocean. Limnol.* **1971**, *17*, 105–123.
48. Provini, A.; Crosa, G.; Marchetti, R. Nutrient export from the Po and Adige river basins over the last 20 years. *Mar. Coast. Eutroph.* **1992**, 291–313. [[CrossRef](#)]
49. Giustini, F.; Brilli, M.; Patera, A. Mapping oxygen stable isotopes of precipitation in Italy. *J. Hydrol. Reg. Stud.* **2016**, *8*, 162–181. [[CrossRef](#)]
50. Marchina, C.; Natali, C.; Bianchini, G. The Po River Water Isotopes during the Drought 530 Condition of the Year 2017. *Water* **2019**, *11*, 150. [[CrossRef](#)]
51. Craig, H. Isotopic variations in meteoric waters. *Science* **1961**, *133*, 1702–1703. [[CrossRef](#)]
52. Marchina, C.; Natali, C.; Fazzini, M.; Fusetti, M.; Tassinari, R.; Bianchini, G. Extremely dry and warm conditions in northern Italy during the year 2015: Effects on the Po river water. *Rend. Lincei Sci. Fis. Nat.* **2017**, *28*, 281–290. [[CrossRef](#)]
53. Barth, J.A.C.; Cronin, A.A.; Dunlop, J.; Kalin, M. Influence of carbonates on the riverine carbon cycle in an anthropogenically dominated catchment basin: Evidence from major elements and stable carbon isotopes in the Lagan River (N. Ireland). *Chem. Geol.* **2003**, *200*, 203–216. [[CrossRef](#)]
54. Bojar, A.V.; Halas, S.; Bojar, H.P.; Trembaczowski, A. Late Permian to Triassic isotope composition of sulfates in the Eastern Alps: Palaeogeographic implications. *Geol. Mag.* **2018**, *155*, 797–810. [[CrossRef](#)]
55. Mayer, B.; Feger, K.H.; Gieseemann, A.; Jäger, H.J. Interpretation of sulfur cycling in two catchments in the Black Forest (Germany) using stable sulfur and oxygen isotope data. *Biogeochemistry* **1995**, *30*, 31–58. [[CrossRef](#)]
56. Raven, M.R.; Adkins, J.F.; Werne, J.P.; Lyons, T.W.; Sessions, A.L. Sulfur-isotopic compositions of individual organic compounds from Cariaco Basin sediments. *Org. Geochem.* **2015**, *80*, 53–59. [[CrossRef](#)]
57. Shawar, L.; Halevy, I.; Said-Ahmad, W.; Feinstein, S.; Boyko, V.; Kamyshny, A.; Amrani, A. Dynamics of pyrite formation and organic matter sulfurization in organic-rich carbonate sediments. *Geochim. Cosmochim. Acta* **2018**. [[CrossRef](#)]
58. Cortecchi, G.; Dinelli, E.; Bencini, A.; Adorni-Braccesi, A.; La Ruffa, G. Natural and anthropogenic SO₄ sources in the Arno river catchment, northern Tuscany, Italy: A chemical and isotopic reconnaissance. *Appl. Geochem.* **2002**, *17*, 79–92. [[CrossRef](#)]
59. Sacchi, E.; Acutis, M.; Bartoli, M.; Brenna, S.; Delconte, C.A.; Laini, A.; Pennisi, M. Origin and fate of nitrates in groundwater from the central Po plain: Insights from isotopic investigations. *Appl. Geochem.* **2013**, *34*, 164–180. [[CrossRef](#)]

60. Martinelli, G.; Dadomo, A.; De Luca, D.A.; Mazzola, M.; Lasagna, M.; Pennisi, M.; Pilla, G.; Sacchi, E.; Saccon, P. Nitrate sources, accumulation and reduction in groundwater from Northern Italy: Insights provided by a nitrate and boron isotopic database. *Appl. Geochem.* **2018**, *91*, 23–35. [[CrossRef](#)]
61. Widory, D.; Petelet-Giraud, E.; Negrel, P.; Ladouche, B. Tracking the sources of nitrates in groundwater using coupled nitrogen and boron isotopes: A synthesis. *Environ. Sci. Technol.* **2005**, *39*, 539–548. [[CrossRef](#)] [[PubMed](#)]
62. Trumbull, R.B.; Slack, J.F. Boron Isotopes in the Continental Crust: Granites, Pegmatites, Felsic Volcanic Rocks, and Related Ore Deposits. *Advances in Isotope Geochemistry* **2018**, 249–272. [[CrossRef](#)]
63. Branson, O. Boron Incorporation into Marine CaCO₃. In *Boron Isotopes; Advances In Isotope Geochemistry*; Marschall, H., Foster, G., Eds.; Springer: Cham, Switzerland, 2018. [[CrossRef](#)]
64. Hemming, N.G.; Hanson, G.N. Boron isotopic composition and concentration in modern marine carbonates. *Geochim. Cosmochim. Acta* **1992**, *56*, 537–543. [[CrossRef](#)]
65. Faure, G.; Assereto, R.; Tremba, E.L. Strontium isotope composition of marine carbonates of middle triassic to early jurassic age, lombardic Alps, Italy. *Sedimentology* **1978**, *25*, 523–543. [[CrossRef](#)]
66. Voshage, H.; Hunziker, J.C.; Hoffman, A.W.; Zingg, A. A Nd and Sr isotopic study of the Ivrea Zone, S. Alps. N-Italy. *Contrib. Mineral. Petrol.* **1987**, *97*, 31–42. [[CrossRef](#)]
67. Spivack, A.J.; Palmer, M.R.; Edmond, J.M. The sedimentary cycle of the boron isotopes. *Geochim. Cosmochim. Acta* **1987**, *51*, 1939–1949. [[CrossRef](#)]
68. Vengosh, A.; Kolodny, Y.; Starinsky, A.; Chivas, A.R.; McCulloch, M.T. Coprecipitation and isotopic fractionation of boron in modern biogenic carbonates. *Geochim. Cosmochim. Acta* **1991**, *55*, 2901–2910. [[CrossRef](#)]
69. Tesi, T.; Miserochi, S.; Acri, F.; Langone, L.; Boldrinc, A.; Hattend, J.A.; Albertazzi, S. Flood-driven transport of sediment, particulate organic matter, and nutrients from the Po. *J. Hydrol* **2013**, *498*, 144–152. [[CrossRef](#)]
70. Marchina, C.; Zuecco, G.; Chiogna, G.; Bianchini, G.; Carturan, L.; Comiti, F.; Engel, M.; Natali, C.; Borga, M.; Penna, D. Alternative Methods to Determine the $\delta^2\text{H}$ - $\delta^{18}\text{O}$ relationship: An Application to Different Water Types. *J. Hydrol* **2020**, *587*. [[CrossRef](#)]
71. Hinderer, M.; Kastowski, M.; Kamelger, A.; Bartolini, C.; Schlunegger, F. River loads and modern denudation of the Alps. A review. *Earth Sci. Rev.* **2013**, *118*, 11–44. [[CrossRef](#)]

